A00-39774

AIAA-2000-4031

DESIGN OF AEROGRAVITY-ASSIST TRAJECTORIES

Wyatt R. Johnson*and James M. Longuski†
School of Aeronautics and Astronautics, Purdue University
West Lafayette, Indiana 47907-1282

Aero-gravity assist (AGA) trajectories are optimized in the sense of maximizing ΔV obtained by the flyby, maximizing aphelion, minimizing perihelion, and minimizing the time of flight (TOF) for a particular destination planet. A graphical method based on Tisserand's criterion is introduced to identify potential AGA trajectories. To demonstrate the application of the theory, patched-conic AGA trajectories are computed to each planet in the Solar System. For an L/D of 7, and a launch V_∞ of 6.0 km/s, Pluto may be reached in 5.5 years using a Venus-Mars-Venus AGA.

Nomenclature

E	=	heliocentric specific orbital energy, km^2/s^2
R	=	semimajor axis of AGA body, km
R_a	=	aphelion distance, km
R_p	=	perihelion distance, km
r_p	=	periapsis at AGA body, km
U	=	nondimensional heliocentric speed
U_∞	=	nondimensional excess velocity
$\mathbf{V}$	=	heliocentric velocity of spacecraft, km/s
$\mathbf{V_{pl}}$	=	velocity of planet with respect to Sun, km/s
$\mathbf{V}_\infty$	=	excess velocity, km/s
α	=	angle between $\mathbf{V}_\infty$ and $\mathbf{V_{pl}}$, rad
θ	=	aerodynamic turn angle, rad
μ	=	gravitational constant, km^3/s^2
ϕ	=	total AGA turn angle, rad

Superscripts

-	=	pre-flyby superscript
+	=	post-flyby superscript

Subscripts

n	=	path index subscript
$\odot$	=	solar

Introduction

GRAVITY assist trajectories have become powerful aids in enabling mankind to explore the Solar System. The famous Voyager II mission depended on gravity assists from multiple planets. The Galileo spacecraft used Earth and Venus in order to reach Jupiter; recently the Cassini spacecraft has used Earth and Venus on its way to Saturn. A much-anticipated mission to Pluto, the Pluto-Kuiper Express, will require high launch energy, along with a Jupiter gravity assist to reach Pluto in 8 years. Many other trajectories to Pluto have been found, requiring up to 4 flyby bodies, with flight times between 10 and 15 years[1] (compared to the Hohmann transfer time of 45 years). However, for a given planet and flyby V_∞, there is a limit to the bending (and thus ΔV) that gravity will supply. Furthermore, with each additional flyby, the total flight time often increases and the required phasing of the planets becomes harder to meet.

Over the years, improvements on the gravity assist idea have been proposed. One of these is to replace the slower conic arcs between planets with faster low-thrust arcs.[2] Though this technique has merit, as the V_∞ of the flyby body increases, the ΔV gained becomes increasingly smaller (as in the case of the conventional gravity assist). Another idea involves flying a lifting body, (e.g., a waverider[3]), through the atmosphere of the flyby planet. Aerodynamic forces can augment the bending angle to arbitrarily large values. Lewis and McRonald[4] contend that the technology exists to build a waverider with L/D ratios greater than 7. The AGA maneuver could dramatically augment the gravity technique.[5,6] An AGA has the added advantage of yielding ΔV increases with higher flyby V_∞s.

Because the turn angle in an AGA is arbitrary, an AGA can perform nearly as well in one flyby as several conventional gravity assists. There will be some energy losses due to drag, but this is more than made up for by the years shaved from the flight time, and the phasing is easier. Preliminary work by Sims[7] shows that with AGA, a spacecraft could reach Pluto in 5 to 7 years, with minimal launch

*Doctoral Candidate, Member AIAA.

†Professor, Associate Fellow AIAA, Member AAS.

energy. Bonfiglio[8] confirms the work of Sims by calculating several AGA trajectories to Pluto with the Satellite Tour Design Program (STOUR), which Bonfiglio modified for the purpose.

In this paper we find the maximum possible ΔV for an AGA maneuver, compute the performance envelope of AGA trajectories, apply a graphical technique to gain further insight into available AGA trajectories, and compute theoretical bounds on the minimum time of flight to each planet.

AGA Equations

A model relating pre and post flyby V_∞s is given by:[9]

$$V_\infty^+ = \left\{ \left(V_\infty^{-2} + \mu/r_p \right) \exp\left[-2\theta/(L/D) \right] - \mu/r_p \right\}^{1/2} \quad (1)$$

For convenience, we nondimensionalize this equation, using $U_\infty \equiv V_\infty{}^2/(\mu/r_p)$ to obtain:

$$U_\infty^+ = \left(U_\infty^- + 1 \right) \exp\left[-2\theta/(L/D) \right] - 1 \quad (2)$$

We calculate the ΔV, and then the more convenient non-dimensional ΔU from

$$\begin{aligned} \Delta V &= V_\infty^{-2} + V_\infty^{+2} - 2V_\infty^- V_\infty^+ \cos(\phi) \\ \Delta U &= U_\infty^- + U_\infty^+ - 2\sqrt{U_\infty^- U_\infty^+}\cos(\phi) \end{aligned} \quad (3)$$

where ϕ is the total turn angle (gravitational and aerodynamic), and is given by

$$\phi = \sin^{-1}\left[(1+U_\infty^-)^{-1} \right] + \sin^{-1}\left[(1+U_\infty^+)^{-1} \right] + \theta \quad (4)$$

Equations 2, 3, and 4 can be combined to yield an expression for ΔU explicitly in terms of U_∞^- and U_∞^+:

$$\begin{aligned} \Delta U \quad &= U_\infty^- + U_\infty^+ - 2\sqrt{U_\infty^- U_\infty^+} \\ &\times \cos\left\{ \sin^{-1}\left[(1+U_\infty^-)^{-1} \right] \right. \\ &+ \sin^{-1}\left[(1+U_\infty^+)^{-1} \right] \\ &\left. + (1/2)(L/D)\ln\left[(U_\infty^- + 1)/(U_\infty^+ + 1) \right] \right\} \end{aligned} \quad (5)$$

Figure 1 shows a graph of Eq. 5 for L/D=15. Because of drag losses, $U_\infty^+ \leq U_\infty^-$ in general. The special case of $U_\infty^- = U_\infty^+$ corresponds to a conventional (pure) gravity assist, and is illustrated separately in Fig. 2. Note that there is a maximum ΔU for all gravity assists. Maximizing Eq. 5 for the pure gravity-assist case, we see that the maximum ΔU is 1, and occurs when $U_\infty = 1$. For the AGA case, however, the maximum ΔU is unlimited and increases with increasing U_∞^-. The rippling effect in Fig. 1 is caused by the $\mathbf{V}_\infty$ being rotated around the planet through several revolutions. The main

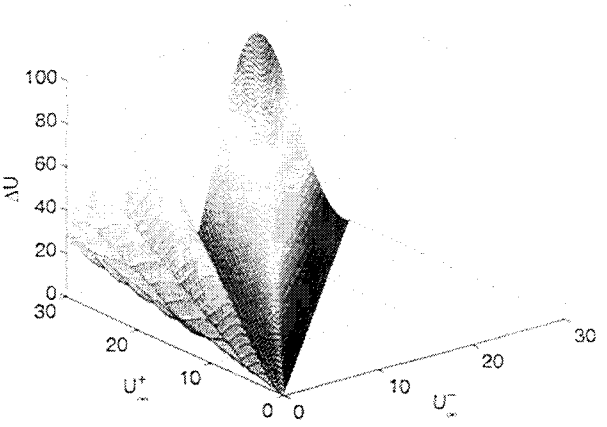

Fig. 1 ΔU **as a function of** U_∞^- **and** U_∞^+ **in an AGA.**

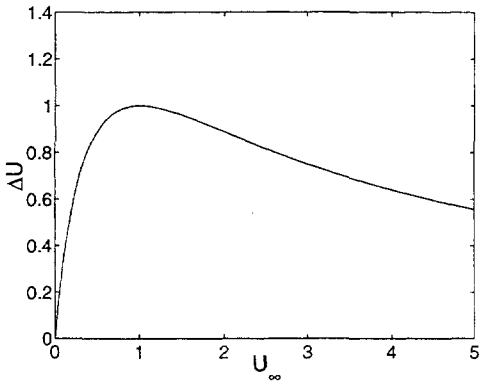

Fig. 2 ΔU **as a function of** U_∞ **in a gravity assist.**

lobe corresponds to the optimal turn angle to maximize ΔU (and hence, ΔV) during the flyby. Further aerodynamic turning decreases U_∞^+ to the first valley, where $\mathbf{V}_\infty^+$ points in the same direction as $\mathbf{V}_\infty^-$. Turning beyond one revolution will again increase the ΔU, but less than before because of drag. Additional revolutions could be completed until $U_\infty^+ = 0$, at which point the spacecraft would be captured in orbit about the gravity-assist planet.

Maximizing ΔV in a Single AGA

To maximize the ΔV obtained by a single AGA, we find an analytic representation of the maximum ΔU, as a function of U_∞^-. It is not obvious from Eq. 5 that ΔU increases almost linearly, but Fig. 1 clearly suggests it. A different approach to this maximization is done by Elices,[10] but with the insight provided by Fig. 1, we find an alternate approximation. Though Elices's approximation has the advantage of being simpler, its accuracy decreases with increasing L/D.

We start with the assumption that for the optimal turn angle, $U_\infty^+ \approx k^2 U_\infty^-$, where k is some

unknown constant. Next, we make this substitution into Eq. 3. We note that as U_∞^- increases, the gravitational turn angles drop out of Eq. 5, and there is a quadratic/logarithmic dependence of U_∞^- on ΔU. We then solve for k in the parameter optimization:

$$\lim_{U_\infty^- \to \infty} \frac{\partial}{\partial k} \Delta U = 0 \tag{6}$$

Because we are assuming U_∞^- is very large, the gravitational turn angle tends towards zero. From Eq. 4, we see that

$$\begin{aligned} \phi &= (1/2)(L/D) \ln \left[(U_\infty^- + 1)/(U_\infty^+ + 1) \right] \\ &\approx -(L/D) \ln k \end{aligned} \tag{7}$$

Equation 6 yields:

$$k - \cos(\phi) - (L/D) \sin(\phi) = 0 \tag{8}$$

This transcendental equation will, in general, have several roots which correspond to the locations in Fig. 1 where a peak is reached. Since we are looking for the maximum peak solution, we pick k to be the value of the largest root. While Eq. 8 can be solved numerically, an explicit form is desired. Intuitively, the optimal turn angle will be somewhat less than π. Furthermore, as $L/D \to \infty$, $k \to 1$. We use the approximations:

$$\begin{aligned} \cos(\phi) &\approx -1 \\ \sin(\phi) &\approx \pi - \phi = \pi + (L/D) \ln k \\ \ln k &\approx (k-1) + (1/2)(k-1)^2 \end{aligned}$$

Two terms are required for the $\ln k$ term to solve for k. (The linear expression is fairly inaccurate except for very high L/D ratios.)

Substituting, we obtain a quadratic expression for k:

$$k^2 + \left[\frac{2}{\left(\frac{L}{D}\right)^2} - 4 \right] k + \left[\frac{2}{\left(\frac{L}{D}\right)^2} - \frac{2\pi}{\frac{L}{D}} + 3 \right] = 0 \tag{9}$$

Solving for the two roots in Eq. 9, we find that one root is always less than 1, and the other is always greater. By inspecting Eq. 7, we see that $k \leq 1$, and thus the higher root is extraneous. Also as $L/D \to \infty$, $k \to 1$, as expected in both cases. Table 1 has a summary of the errors in these three approximations (Elices, the transcendental, and the quadratic) for U_∞^-s ranging from 0 to 30.

In the quadratic and transcendental formulations, ΔU is linearly related to U_∞^- by:

$$\Delta U = U_\infty^- \left[1 - 2k \cos(\phi) + k^2 \right] \tag{10}$$

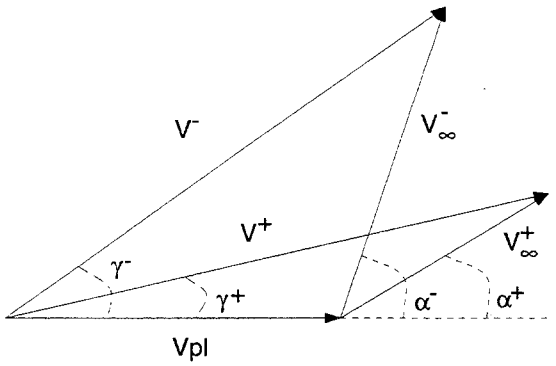

Fig. 3 The AGA vector diagram.

Unsurprisingly, the transcendental version is the most accurate at all L/D ratios. At low L/D ratios, Elices's approximation is the next most accurate. At about $L/D = 4$, the quadratic begins to do better. Since the Taylor series expansion was done about $k = 1$ (which is the case for $L/D \to \infty$), it is expected that the two methods developed here asymptotically reach zero error as L/D increases.

The first error listed in Table 1 is the maximum percent error in the $0 \leq U_\infty \leq 30$ comparison range. In all cases the largest errors occur at high values of U_∞; at high U_∞^- and low L/D, none of the estimators are accurate. A more representative error is the mean error, which shows the average error for all examined U_∞ is fairly small. Finally, the mean squared error (MSE) is listed for all cases.

Optimizing for Perihelion or Aphelion

Clearly AGA can potentially yield dramatic improvements in attainable ΔV over conventional gravity assists. But unless a maximum ΔV AGA makes it easier to reach a desired destination, the attainable ΔV is useless. The turn angle that results in the maximum ΔV may not necessarily be the optimal turn angle for reaching the next body. Indeed, one of the major points of the maximum ΔV theory is to provide a benchmark for practical AGAs (e.g., AGAs that actually get the spacecraft somewhere).

To this end, we examine optimizing the turn angles about the planets to maximize the spacecraft's aphelion, or to minimize its perihelion, depending on if the target body is farther from or closer to the Sun. The spacecraft will then be able to reach any body in the Solar System between these two bounds. The derivations that follow assume circular coplanar planetary orbits. Figure 3 presents a vector diagram of the AGA maneuver.

Table 1 Percent error in approximating maximum AGA ΔU by different estimators

L/D	Elices[10]			Transcendental			Quadratic		
	Max	Mean	MSE[a]	Max	Mean	MSE[a]	Max	Mean	MSE[a]
1	74.4	17.1	3.3	69.0	3.7	0.7	55.3	44.5	21.6
2	61.9	3.7	0.4	58.4	1.4	0.3	68.8	23.3	5.7
3	53.4	3.2	0.3	49.7	0.7	0.2	55.2	6.8	0.6
4	46.9	3.6	0.2	43.0	0.4	0.1	46.3	2.5	0.2
5	41.5	3.6	0.2	37.8	0.3	0.1	40.0	1.0	0.1
10	23.2	1.1	0.1	23.3	0.3	0.0	23.7	0.2	0.0
15	17.8	6.5	0.5	16.7	0.4	0.0	16.8	0.0	0.0

[a] Mean Squared Error

L/D=∞ case

The simplest case to consider is $L/D = \infty$ where the spacecraft would not lose any V_∞ due to drag during the aerodynamic turning. This case puts a theoretical upper/lower bound on what *any* AGA can accomplish. No matter how waverider technology progresses, a waverider will never be able to outperform this limit.

The arrival V_∞ at the AGA planet is computed as:

$$\begin{aligned} V_{\infty,2}^2 &= V_2^2 + V_{pl,2}^2 - 2V_{pl,2}V_2\cos(\gamma_2) \\ &= V_2^2 + V_{pl,2}^2 - 2(R_1/R_2)V_{pl,2}\cos(\gamma_1) \\ &= V_1^2 + V_{pl,2}^2 - 2(R_1/R_2)V_{pl,2}\cos(\gamma_1) \\ &\quad +2\mu_\odot\left(R_2^{-1} - R_1^{-1}\right) \\ &= V_{pl,1}^2 + V_{pl,2}^2 + V_{\infty,1}^2 - 2(R_1/R_2)V_{pl,1}V_{pl,2} \\ &\quad +2\mu_\odot\left(R_2^{-1} - R_1^{-1}\right) + 2V_{\infty,1}V_{pl,1}\cos(\alpha_1) \\ &\quad -2(R_1/R_2)V_{\infty,1}V_{pl,2}\cos(\alpha_1) \qquad (11) \end{aligned}$$

Now that we have an expression for the arrival V_∞ at the AGA planet in terms of departure conditions at Earth, we can find the optimum α_1 to maximize $V_{\infty,2}$. The first and second derivative rules tell us that $\alpha_1 = 0°$ if $R_2 > R_1$, or $\alpha_1 = 180°$, if $R_2 < R_1$. In the $R_2 > R_1$ case, we maximize aphelion, and minimize perihelion in the other.

With a L/D of ∞, a spacecraft can turn any desired turn angle without losing V_∞. The Hohmann transfer shows that a tangential ΔV is optimum for maximizing aphelion or minimizing perihelion. Thus, the optimum turn angle in this case makes the $\mathbf{V}_\infty$ parallel to the planet's velocity vector (this is not true for the finite L/D case, as rotating the $\mathbf{V}_\infty$ also decreases its magnitude). Since for a tangential departure, maximizing heliocentric velocity is equivalent to maximizing aphelion (and similarly, minimizing heliocentric velocity is equivalent to minimizing perihelion), we know that $V_2^+ = V_{pl,2} \pm V_{\infty,2}$.

Thus, maximum aphelion or minimum perihelion can be computed as:

$$R_{a,p} = R_2\left[U/(2-U)\right] \qquad (12)$$

Equation 12 is derived assuming the spacecraft departs Earth and executes an AGA at the next planet in its path sequence. However, because (as shown in Eq. 11) tangential Earth departures are optimal in this sense, and because tangential AGA planet departures are optimal, we can patch several of these trajectories together to get the optimal multi-body trajectory. This is done by departing each body tangentially as to maximize the arrival V_∞ at the next body. When the spacecraft arrives at the next body, it turns so it leaves tangentially to go on to the next planet.

Finite L/D case

Of course, infinite L/D ratios are impossible. A parameter optimization problem can be set up for the finite L/D case similar to the infinite L/D case. However, V_∞^+ is now a function of V_∞^- and θ. Launching tangentially from Earth is also not necessarily optimal. For a single-body AGA, maximizing aphelion or minimizing perihelion can be formulated as a two-dimensional parameter optimization problem for a given L/D and launch V_∞. Each additional AGA body in the path sequence adds another dimension to the problem (the aerodynamic turning angle for that planet). An analytic solution appears intractable, so a numerical solution is calculated. The results are presented in Figs. 4 and 5.

Figure 4 illustrates the maximum aphelion and minimum perihelion possible with a single AGA at Venus for several different L/D ratios. The Venus Gravity Assist (VGA) and Venus Aerogravity Assist (VAGA) contours begin at a launch V_∞ of 2.5 km/s, which corresponds to the Hohmann transfer. Note that at this launch V_∞, it is impossible to increase aphelion, since the spacecraft arrives at Venus with its $\mathbf{V}_\infty$ aligned with the velocity vector of Venus (i.e., $\alpha = 0$). However, it is still possible to decrease perihelion. The more turning that can be accomplished (i.e., the higher the L/D ratio), the lower the

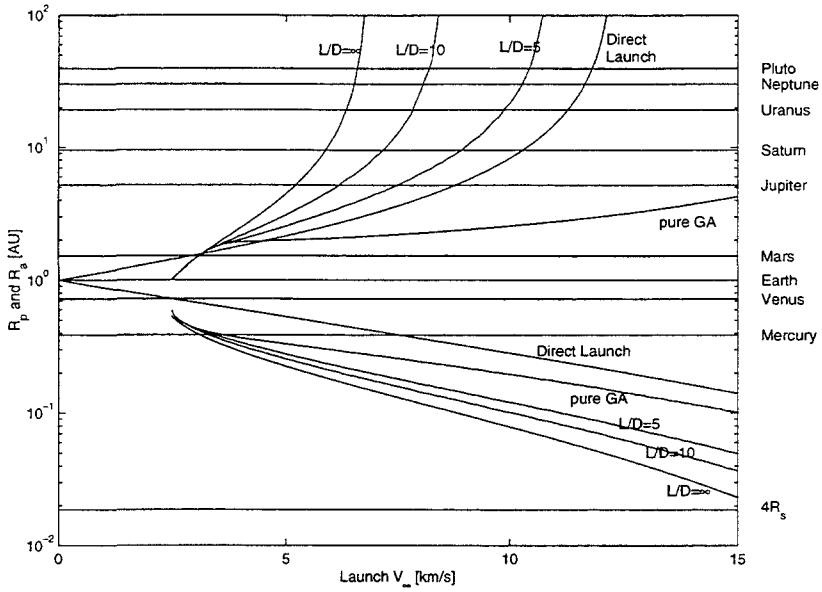

Fig. 4 Maximizing aphelion or minimizing perihelion using a single Venus aerogravity assist (VAGA).

perihelion can be. The ability to decrease perihelion for the Hohmann transfer is the cause for the apparent discontinuity in Fig. 4 — the Hohmann results in a perihelion at Venus; but we can immediately get additional bending to decrease it even further.

As the launch V_∞ increases, so does the arrival V_∞ at Venus. Furthermore, α also increases. This makes it possible to increase aphelion by rotating the $\mathbf{V}_\infty$ back towards $\alpha = 0$. For launch V_∞s less than 3.2 km/s, a pure VGA is able to achieve maximum turning (without overturning the $\mathbf{V}_\infty$). Thus, an AGA is not needed.

But for launch V_∞s higher than 3.2 km/s, a VAGA more effectively increases aphelion. A pure VGA can not even get to Jupiter for a launch V_∞ of 15 km/s. For a high launch V_∞, there is a correspondingly high α at the VGA. But with high arrival V_∞ at Venus, the maximum turn angle is insufficient to rotate the $\mathbf{V}_\infty$ enough to increase the spacecraft's heliocentric velocity (and therefore, energy). A VAGA does not suffer this disadvantage, since the $\mathbf{V}_\infty$ can be rotated to an arbitrary direction. The aerodynamic portion of a turn is responsible for most of the turning at high arrival V_∞s, unlike low arrival V_∞s where gravity dominates.

Since Figs. 4 and 5 represent aphelion and perihelion distances, the points where a contour intersects a planet imply the spacecraft arrives tangentially. Also, the $L/D = \infty$ case must always depart Venus tangentially, since this provides the extremal heliocentric velocity. Therefore, points where the $L/D = \infty$ contour intersect a planet are all identical to Hohmann transfers from Venus to that planet, and may have fairly lengthy TOFs. For all finite L/D contours, the departure α will be somewhat larger. Thus, Venus will not be at perihelion (if traveling upwell) or aphelion (if traveling downwell). Although the TOFs will be shorter, they are not much more so if traveling to the outer planets, and come at the cost of increased launch V_∞.

In many ways, Mars behaves oppositely to Venus. Figure 5 illustrates the Mars Gravity Assist (MGA) and the Mars Aerogravity Assist (MAGA). At the Hohmann launch V_∞, it is impossible to decrease perihelion; however, aphelion can still be increased. Furthermore, the MGA is capable of full turning for launch V_∞s less than 3.2 km/s. The arc where gravity alone is sufficient is smaller than that of Venus, because Mars has lower gravity. Because of this lower gravity, the MGA can barely rotate the $\mathbf{V}_\infty$ at higher arrival V_∞s. However, the MAGA is still able to, since the departure direction is unconstrained. This is the reason behind the large gap in increasing aphelion between the pure MGA case and the $L/D = 5$ case. At the launch V_∞ for an MGA to reach Jupiter, a MAGA is easily capable of escaping the Solar System. In other words, a single MAGA allows a spacecraft to reach Jupiter instead of requiring the traditional 2 or 3 flybys of other planets.

A MAGA is also more capable of decreasing perihelion at higher launch V_∞s than a VAGA. Decreasing perihelion is equivalent to reducing heliocentric velocity during a flyby. For any gravity-assist body, the goal is to rotate the spacecraft's $\mathbf{V}_\infty$ to be paral-

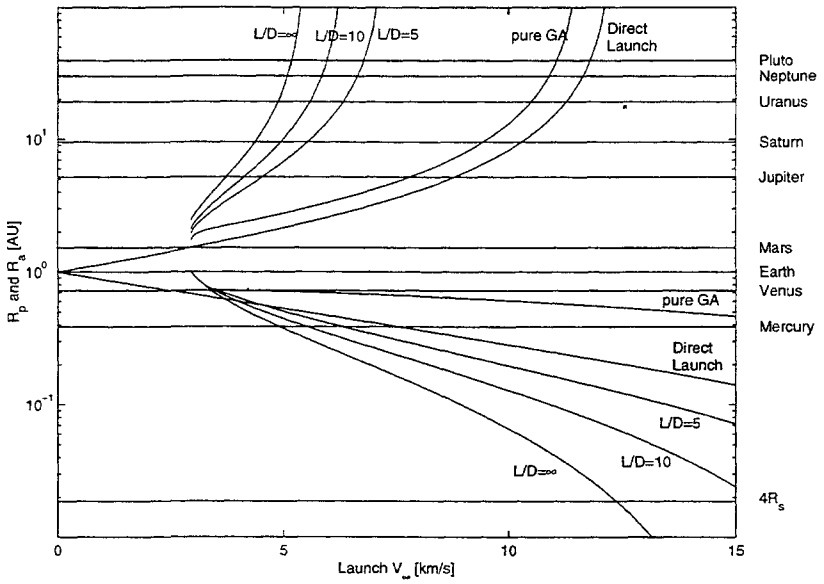

Fig. 5 Maximizing aphelion or minimizing perihelion using a single Mars aerogravity assist (MAGA).

lel, and opposite in direction to the planet's velocity vector. Since the departure direction is arbitrary for an AGA, and the heliocentric velocity of Mars is much smaller than that of Venus, a MAGA is able to reduce perihelion more than a VAGA can, for the same flyby V_∞.

When there are more than one or two AGA planets to consider, this graphical method becomes cumbersome, and does not provide much insight. Another drawback is that this approach does not provide the arrival $\mathbf{V}_\infty$, nor does it provide the TOF. An alternate method is developed instead.

E-R_p Analysis

A graphical tour design method based on Tisserand's criterion was developed to aid in searching for paths for the Europa Orbiter mission.[11,12] If we assume that satellites are in circular, coplanar orbits around a central body, then two orbital elements completely describe the shape of the orbit. For the Europa Orbiter case, period and periapsis radius were selected. We use specific orbital energy instead of period, since many conic arcs to the outer planets are hyperbolic with respect to the Sun. Since these two quantities provide the orbit shape, the flyby conditions are known when that orbit crosses a given body's path. In particular, the arrival V_∞ is known for a given E, R_p, and flyby planet. From Fig. 3, we have that:

$$\begin{aligned} {V_\infty}^2 &= V_{pl}^2 + V^2 - 2V_{pl}V\cos(\gamma) \\ &= V_{pl}^2 + 2E + 2\mu_\odot/R - 2V_{pl}V\cos(\gamma) \\ &= V_{pl}^2 + 2E + 2\mu_\odot/R \\ &\quad -2(R_p/R)V_{pl}\sqrt{2E + 2\mu_\odot/R} \\ &= 2E + 3\mu_\odot/R - 2(R_p/R) \\ &\quad \times\sqrt{2(\mu_\odot/R)\,(E + \mu_\odot/R_p)} \end{aligned} \tag{13}$$

In pure gravity assists, the pre and post V_∞s are the same, but the orbits (which are points on an E-R_p plot) are different. This is graphically depicted as following constant V_∞ contours on an E-R_p plot, as shown in Fig. 6. The distance on a contour that can be traversed by a single flyby depends (in part) on the radius of the flyby body (i.e., when a flyby approaches the surface, further turning is not possible). The tick marks (dots) on the plot denote contour distance at maximum turning. This plot illustrates that Mars is not a very effective gravity-assist body, since its tick marks are very close together. On the other hand, Jupiter's tick marks are spread out, and therefore much more capable of altering a spacecraft's orbit.

An AGA further spreads out the tick marks. Consider the hypothetical $L/D = \infty$ case where the $\mathbf{V}_\infty$ can be turned to any desired direction. This corresponds to moving the tick marks to the endpoints of the contours (or simply removing them). Finite L/D values complicate matters because the V_∞ does not remain constant. As the aerodynamic turn angle increases, the V_∞^+ decreases. However, this loss may be worthwhile since the tick mark constraint is no longer valid. Putting this all together, a sample trajectory to Pluto is depicted in Fig. 7.

In Fig. 6, the V_∞ contours start at the lower-right

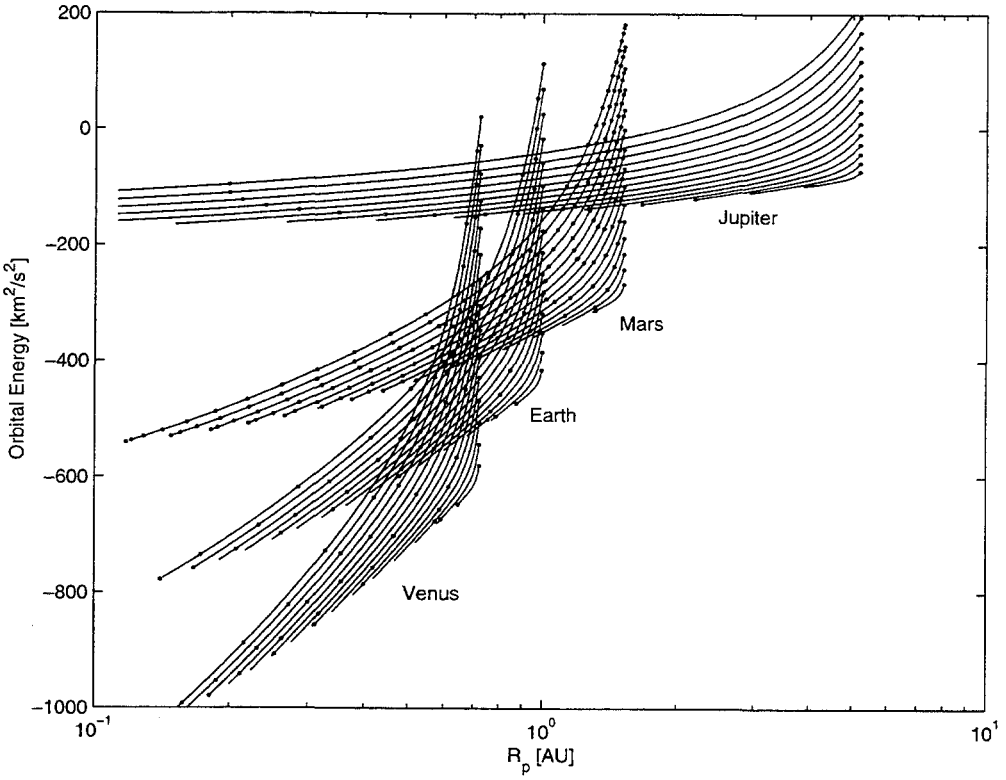

Fig. 6 The E-R_p plot.

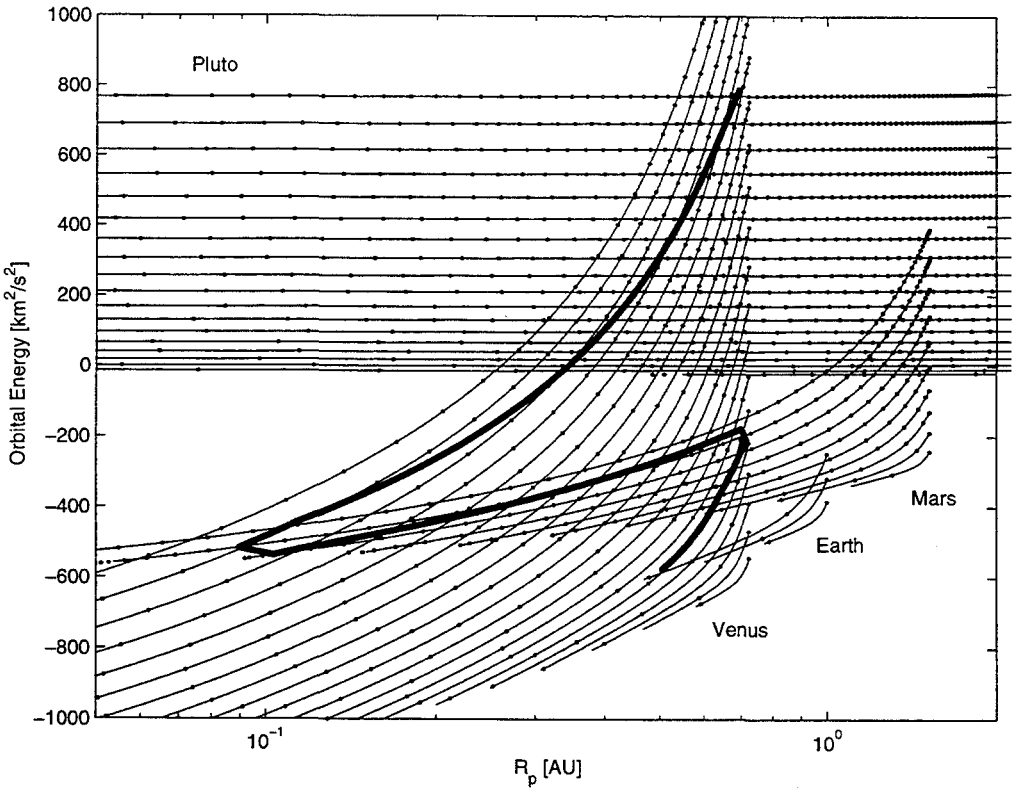

Fig. 7 Illustration of an EVMVP trajectory using AGA.

corner at $V_\infty = 1$ km/s for each of the planets. The spacing between contours is also 1 km/s. In Fig. 7, the contour spacings are at 2 km/s for better clarity. This figure depicts a trajectory from Earth to Pluto using AGAs, with a launch V_∞ of 6 km/s. This launch condition is also on a Venus contour — meaning that the spacecraft can coast from Earth to Venus. If phasing works out, Venus will be there when the spacecraft reaches Venus's orbit. Next, the spacecraft goes on to Mars via a Venus AGA (VAGA). This is graphically depicted as proceeding up the first arc along the Venusian contours. If a VGA were done instead, the spacecraft would be limited in its turning (it can cross only one tick mark). With an AGA, the spacecraft can get some "free" gravitational turning; but the rest of the turning will result in loss of V_∞. In this case, the spacecraft arrives at Venus with a V_∞ of about 12.3 km/s, but leaves Venus with a V_∞ of only 10.7 km/s. This allows the spacecraft to arrive at Mars with a V_∞ of 18.9 km/s. The spacecraft performs another AGA, which lowers its Mars V_∞ to 16.0 km/s, but this allows its perihelion to be drastically pumped down to 0.086 AU. The spacecraft coasts to Venus, where a final VAGA pumps up the heliocentric energy to a hyperbolic orbit. From there, the spacecraft can reach Pluto.

The E-R_p plot provides a valuable tool for examining GA or AGA trajectories. However, the decaying V_∞ in the AGA maneuver complicates the interpretation of the E-R_p plot. For this reason, a computer program was written to search through the E-R_p contours to find the shortest TOF trajectory from Earth to every other planet. The program calculates both GA and AGA cases for any number of flyby bodies. But because of the circular, coplanar assumption, and the lack of phasing (timing) considerations, any hypothetical trajectory still needs to be verified by other means.

Because the orbital state — specific energy and perihelion — is a continuous vector, we discretize the E-R_p plot into a collection of nodes. The orbital state vector after a flyby is then mapped to the nearest node. Thus, the finer the discretization, the smaller the error in the algorithm. There are up to 4 possible coast arcs from one planet to another for each point in the E-R_p plot[11] (only 2 possible arcs for hyperbolic trajectories). All possible arcs are considered, keeping the direction of the trajectory consistent for each arc. There are literally billions of trajectories that must be considered. To drastically cut back on search time, while ensuring each optimal trajectory is found, we employ the Viterbi algorithm.[13] This algorithm finds the minimum TOF path between any desired initial and final condition in the minimal number of comparisons.

Table 2 Fastest potential AGA trajectories to Mercury with L/D=7 (ignoring phasing). The TOF is given in years.

V_∞	Mercury	
	Path	TOF
3	EVEVY	0.79
4	EVY	0.37
5	EVY	0.30
6	EVY	0.27

The AGA results for Mars and Venus are unremarkable, since no gravity assists are needed to reach them. (The one exception being a launch V_∞ higher than the Earth-Venus Hohmann, but lower than the Earth-Mars Hohmann. In this case, a Venus flyby is required to get to Mars.) The optimal trajectory from Earth to Mercury involves at least one flyby at Venus. For launch V_∞s higher than 4, the TOF savings with AGA is minimal. A summary of results for trajectories to Mercury is presented in Table 2.

For a launch V_∞ of 3 km/s, a single VAGA is insufficient to reach Mercury; furthermore, it is impossible to reach Mercury with only 2 flybys. The fastest potential 3-flyby trajectory to Mercury uses a Venus-Earth-Venus combination of AGAs for a TOF of 0.79 years. Additional flybys beyond the third increases the TOF, and thus are unnecessary. For launch V_∞s of 4 km/s or higher, a single VAGA is sufficient to reach Mercury. The TOF cannot be improved with additional flybys.

The biggest advantage of AGA is in missions to the outer planets. A summary of results is shown in Table 3. Blank areas mean that no such trajectory is possible (due to insufficient launch energy). For example, no trajectory to Jupiter using only 1 or 2 flyby bodies exists for a launch V_∞ of 3 km/s.

Since this analysis does not take into account phasing (however, it does allow for resonant flybys), the existence of a trajectory that returns to a given planet is not guaranteed. In general, the greater the number of times a given planet is used (excluding resonant flybys), the less likely such a trajectory will exist.

Our algorithm allows for an AGA at all planets except Mercury and Pluto (which do not have appreciable atmospheres). Interestingly enough, the time-optimal trajectories rely most heavily on Venus and Mars, and only occasionally use Earth. For many of the cases, the optimal trajectory is an alternating series of Venus, Earth, and Mars AGAs until

Table 3 Fastest potential AGA trajectories to the outer planets with L/D=7 (ignoring phasing). The TOF is given in years.

V_∞	Jupiter		Saturn		Uranus		Neptune		Pluto	
	Path	TOF	Path	TOF	Path	TOF	Path	TOF	Path	TOF
	EVEMJ	1.99	EVEMS	3.53	EVEMU	8.21	EVEMN	15.33	EVEMP	23.08
3	EVEVMJ	1.64	EVEVMS	2.43	EVEVMU	4.24	EVEVMN	6.35	EVEVMP	8.21
	EVEVEMJ	1.56	EVEVMVS	2.20	EVEVMVU	3.46	EVEVMVN	4.91	EVEVMVP	6.18
	EVMJ	2.20	EVMS	5.61						
4	EVEMJ	1.43	EVEMS	2.44	EVMVU	4.71	EVMVN	7.21	EVMVP	9.44
	EVEMVJ	1.36	EVEMVS	1.92	EVEMVU	3.20	EVEMVN	4.65	EVEMVP	5.93
	EVEMVEJ	1.32	EVEMVES	1.87	EVEMVEU	3.14	EVEMVEN	4.58	EVEMVEP	5.85
	EMJ	2.46								
	EVMJ	1.46	EVMS	2.61	EVMU	5.52	EVMN	9.14	EVMP	12.45
5	EVEMJ	1.24	EVMVS	2.08	EVMVU	3.53	EVMVN	5.18	EVMVP	6.63
	EVEMVJ	1.23	EVEMVS	1.78	EVEMVU	3.04	EVEMVN	4.49	EVEMVP	5.76
	EMJ	1.68	EMS	3.64	EMU	14.16				
6	EVMJ	1.27	EVMS	2.21	EMVU	4.41	EMVN	6.96	EMVP	9.23
	EVEMJ	1.11	EVMVS	1.74	EVMVU	3.00	EVMVN	4.45	EVMVP	5.72

the destination planet is reached. Because the inner planets have such low semimajor axes compared to the outer planets, using them exclusively (since we can get arbitrary bending at them) is better than hoping all the outer planets line up right. For example, the best trajectory to Pluto with a launch V_∞ of 6 km/s uses a Venus-Mars-Venus-Mars series of AGAs, as opposed to using Jupiter, Saturn, Uranus, or Neptune (even though AGAs are also allowed at these planets). While Jupiter is a powerful gravity-assist planet, it is too far away to effectively compete with the inner planets. Another factor evident from examining Fig. 6 is that if Jupiter is used to pump up a spacecraft's energy, then its semimajor axis is greatly increased. This lengthens the size and TOF of the conic arc to the next planet, and thus, Jupiter is not used. This means that we do not have to depend on phasing with Jupiter to get to the outer planets — only on the phasing of Venus, Earth, and Mars.

Considering trajectories to Pluto for a launch V_∞ of 6.0 km/s, we see that adding a 3rd flyby lowers the TOF to 5.7 years. This trajectory is, in fact, the EVMVP discussed previously. However, the actual TOF may be much shorter, since Pluto is currently about 30 AU away from the Sun, while our algorithm assumes a constant semimajor axis of approximately 40 AU.

This trajectory was examined in more detail using STOUR for a 40-year launch window (2000-2040) and launch V_∞s ranging from 4.0 km/s to 6.0 km/s. The results are shown in Fig. 8. The trajectory is indicated by the PATH label, where the number n corresponds to the nth planet from the Sun. The LIFT/DRAG field gives the L/D ratios used at each flyby planet. In this case, an L/D=7 was used during the VMV. Finally, the plot itself is comprised of several letters. Each of these represents a trajectory with the indicated launch date and TOF. The letter itself is an index for the launch V_∞s that are searched. In this case, an "A" represents a launch V_∞ of 4.00 km/s; a "B" represents a launch V_∞ of 4.50 km/s, and so on.

With the given conditions, the fastest trajectory to Pluto has a launch V_∞ of 6.0 km/s, and takes only 5.5 years! If we use a launch V_∞ of only 5.5 km/s instead, we can get there only slightly later. Furthermore, these trajectories are possible every few years. These extremely low TOF trajectories to Pluto begin to disappear as Pluto moves further away. Even with a lower L/D ratio of 5, the VMV trajectory still yields short TOFs, somewhat less than a year longer than the $L/D = 7$ case. Earlier work by Bonfiglio yielded AGA trajectories to Pluto that either took 5 years longer for the same launch energy, or took 4 years longer for an increased launch energy of 7 km/s. Clearly, the E-R_p graphical method is a powerful tool.

Another mission of interest is the Solar Probe which will study the Sun from as close as 4 solar radii. Reducing perihelion by that much by a direct launch is very expensive, requiring a 25 km/s launch V_∞ to offset the Earth's heliocentric velocity. A pure GA trajectory to achieve the same goal requires that the last gravity assist has a flat contour, with tick marks far enough apart. Examining Fig. 6, we see that the only practical choice for pure GA is Jupiter. In theory, any planet could be used, but several resonances are required, which drives up the TOF to unreasonable values. Previously, we noted that the VMV AGA trajectory to Pluto as graphed in Fig. 7 has a very small perihelion of 0.086 AU after the MAGA. The second VAGA increases energy and perihelion to get to Pluto. However, suppose we use the second VAGA to reduce energy and perihelion. Trajectories to 4 solar radii are computed

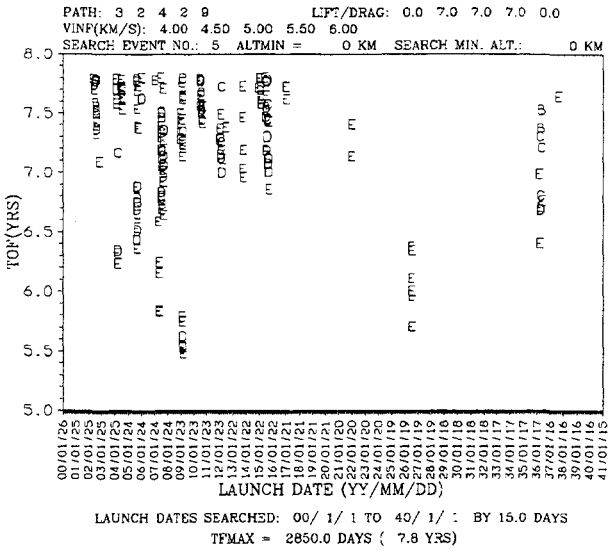

Fig. 8 VMV AGA trajectories to Pluto.

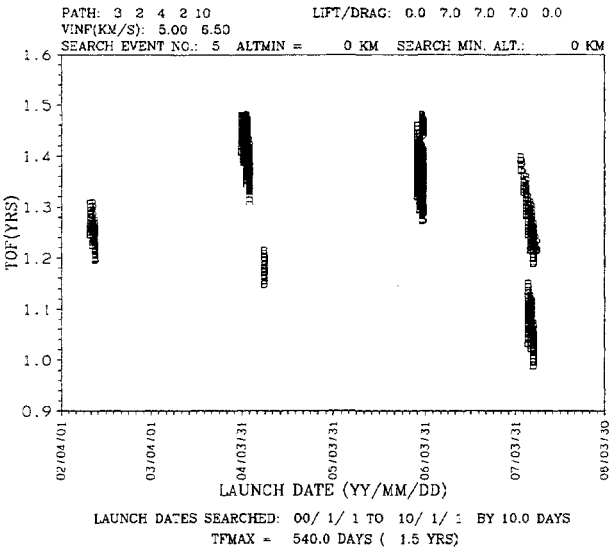

Fig. 9 VMV AGA trajectories to 4 solar radii.

using STOUR, and are shown in Fig. 9. Trajectories with launch V_∞s as low as 4.50 km/s are possible, the fastest having a 2-year TOF. For a launch V_∞ of 5.00 km/s to 6.50 km/s, many trajectories have TOFs under 1.5 years. The quickest of these has a TOF just under a year.

The proposed GA Solar Probe mission has a TOF of around 6 years, and an aphelion of Jupiter's distance of 5.2 AU. The probe would have at least a 4-year period, with an extremely fast perihelion flyby. On the other hand, the AGA trajectories in Fig. 9 all have perihelia near Venus. This corresponds to about a 75-day period, with a slower flyby. The AGA trajectories thus allow for more science return, since the spacecraft would return to the Sun more frequently. As with the VMV trajectories to Pluto, launch opportunities for a solar mission exist every few years.

Discussion

Previously, we found the optimal atmospheric turn angle to maximize ΔV; but, we also know that this $\mathbf{\Delta V}$ may not be pointing in the right direction to get to the next planet. We can find the necessary conditions for a maximum AGA ΔV to accomplish this by inspecting the E-R_p plot (Fig. 6).

If an AGA begins near one of the endpoints of a V_∞ contour (far lower-left or far upper-right), then a maximum ΔV AGA would drive the spacecraft toward the other endpoint (but at a lower contour, since some V_∞ is lost). However, a maximum ΔV AGA maneuver that begins near the middle of a V_∞ contour would follow the contour in one direction, then backtrack (overturn), only to end up near where the maneuver began. (This results in a large change in the spacecraft's true anomaly, but little change in the shape of the orbit itself. A smaller turn angle gives an equivalent turn, but with less loss of V_∞.) Thus, the most efficient ΔVs possible with an AGA are the ones that arrive and depart the flyby body nearly tangentially. The limiting case occurs when $L/D = \infty$, where the spacecraft arrives *and* departs tangentially. The near-tangential arrival/departure condition is met in the previously discussed EVMVP trajectory of Fig. 7. As seen in the figure, all 3 AGAs are located near the endpoint of a V_∞ contour. However, arriving *or* departing a contour near an endpoint is insufficient for maximizing ΔV for a given L/D. Because the optimal turn angle is a function of L/D, higher L/D ratios permit greater travel along the V_∞ contours. For $L/D = 7$, Eqs. 7 and 9 yield $\phi \approx 174$ degrees, so the AGA maneuver travels through about 97% of a V_∞ contour. Clearly, the AGAs in Fig. 7 are not ΔV-maximum, since the AGAs begin in the middle of a contour. However, due to the geometry of the contours, maximum-ΔV AGAs are not possible for the EVMVP case at higher L/D ratios; i.e., an AGA is capable of providing a ΔV in excess of what is optimal for reaching the next body. Therefore, a lower L/D ratio exists such that a maximum ΔV AGA is possible and optimal for a specific maneuver. The AGAs in Fig. 7 do turn the maximum amount without overturning. Moreover, even when a maximum ΔV trajectory exists, it may not be time-optimal. From Fig. 7, we see that an EVMP is possible using a maximum ΔV AGA with a Mars V_∞^- of 10 km/s. However, from Table 3, we know that the EVMVP is faster than the EVMP. Even with a series of AGAs that do not use 100% of the possible ΔV, the tra-

jectory can be faster than any comparable pure GA trajectory.

Conclusions

An AGA can potentially yield much higher ΔVs than a pure gravity assist, and the E-R_p plot shows when it is possible. The real power of AGA is apparent when multiple AGA flybys are used, especially when one body acts as a V_∞-leveraging maneuver for another (such as a VMV or MVM). These trajectories allow for extremely fast low-energy missions.

As seen from the E-R_p analysis, the Earth is not used as often for AGA because it has only a moderate effect on the orbit shape. On the other hand, Mars and Venus can be quite effective. Venus is typically most useful in changing the orbital energy of a spacecraft, while Mars is typically most useful in changing a spacecraft's perihelion. Earth can do both, but neither quite as well as Mars or Venus. The outer planets are too far away to be useful as AGA bodies.

AGA provides three significant advantages. First, trajectories do not have to rely on phasing of the outer planets (aside from the target) but only on Venus, Earth, and Mars. Second, TOFs are small. Since the initial phase of an AGA trajectory will usually rely only on Venus and Mars, the time required to build up the spacecraft's orbital energy is kept to a minimum. Finally, fast trajectories to all planets exist using low launch energy.

The AGA technique provides exciting new trajectories to difficult targets in the Solar System. For example, Pluto can be reached in only 5.5 years using a VMV AGA, for a L/D of 7, with a launch V_∞ of 6.0 km/s. The trajectories presented here supply compelling reasons to develop high L/D hypersonic vehicles (such as the waverider). The development of AGA technology will enable deep space exploration at low launch energy and for short flight time.

References

[1]Sims, J., Staugler, A., and Longuski, J., "Trajectory Options to Pluto via Gravity Assists from Venus, Mars, and Jupiter," *Journal of Spacecraft and Rockets*, Vol. 34, No. 3, May-June 1997, pp. 347–353.

[2]Petropoulos, A., Longuski, J., and Vinh, N., "Shape-Based Analytic Representations of Low-Thrust Trajectories for Gravity-Assist Applications," AAS Paper No. 99-337, AAS/AIAA Astrodynamics Specialist Conference, Girdwood, Alaska, Aug. 1999.

[3]Nonweiler, T., "Aerodynamic Problems of Manned Space Vehicles," *Journal of the Royal Aeronautics Society*, Vol. 63, Sept. 1959, pp. 521–528.

[4]Lewis, M. and McRonald, A., "Design of Hypersonic Waveriders for Aeroassisted Interpanetary Trajectories," *Journal of Spacecraft and Rockets*, Vol. 29, No. 5, Sept.-Oct. 1992, pp. 653–660.

[5]Randolph, J. and McRonald, A., "Solar System 'Fast Mission' Trajectories Using Aerogravity Assist," *Journal of Spacecraft and Rockets*, Vol. 29, No. 2, March-April 1992, pp. 223–232.

[6]McRonald, A. and Randolph, J., "Hypersonic Maneuvering for Planetary Gravity Assist," *Journal of Spacecraft and Rockets*, Vol. 29, No. 2, March-April 1992, pp. 216–222.

[7]Sims, J., "Delta-V Gravity-Assist Trajectory Design: Theory and Practice," Ph.D. Thesis, School of Aeronautics and Astronautics, Purdue University, West Lafayette, IN, Dec. 1996.

[8]Bonfiglio, E., "Automated Design of Gravity-Assist and Aerogravity-Assist Trajectories," Master's Thesis, School of Aeronautics and Astronautics, Purdue University, West Lafayette, IN, Aug. 1999.

[9]Anderson, J., Lewis, M., Kothari, A., and Corda, S., "Hypersonic Waveriders for Planetary Atmospheres," *Journal of Spacecraft and Rockets*, Vol. 28, No. 4, July-Aug. 1991, pp. 401–410.

[10]Elices, T., "Maximum ΔV in the Aerogravity Assist Maneuver," *Journal of Spacecraft and Rockets*, Vol. 32, No. 5, Sept.-Oct. 1995, pp. 921–922.

[11]Strange, N. and Longuski, J., "A Graphical Method for Gravity Assist Trajectory Design," AIAA Paper No. 2000-4030, Denver, Colorado, Aug. 2000.

[12]Heaton, A., Strange, N., Longuski, J., and Bonfiglio, E., "Automated Design of the Europa Orbiter Tour," AIAA Paper No. 2000-4034, Denver, Colorado, Aug. 2000.

[13]Viterbi, A., "Error bounds for convolutional codes and an asymptotically optimal decoding algorithm," *IEEE Transactions on Information Theory*, Vol. IT-13, April 1967, pp. 260–269.